

Photocatalytic Degradation of Nitrobenzene Using Nanocrystalline TiO₂ Photocatalyst Doped with Zn Ions

Edgar Alonso Reynoso-Soto,^{a,*} Sergio Pérez-Sicairos,^a Ana Patricia Reyes-Cruzaley,^a Christian Leonardo Castro-Riquelme,^a Rosa María Félix-Navarro,^a Francisco Paraguay-Delgado,^b Gabriel Alonso-Núñez,^c Shui Wai Lin-Ho^a

^a Centro de Graduados e Investigación. Instituto Tecnológico de Tijuana. Apdo. Postal 1166. Tijuana, B. C. 22000, México.

^b Centro de Investigación en Materiales Avanzados. Miguel de Cervantes 120 Apdo. Postal 31109, Chihuahua, México.

^c Centro de Nanociencias y Nanotecnología. Universidad Nacional Autónoma de México. Km. 107 Carretera Tijuana-Ensenada. Apdo. Postal 356 Ensenada, B. C. 22800, México.

Received February 13, 2013; Accepted May 31, 2013.

Abstract. Photocatalysis is a method widely used in the degradation of organic pollutants of the environment. The development of new materials is very important to improve the photocatalytic properties and to find new applications for TiO₂ as a photocatalyst. In this article we reported the synthesis of a photocatalyst based on TiO₂ doped with Zn²⁺ ions highly efficient in the degradation of nitrobenzene. The results of photocatalytic activity experiments showed that the Zn²⁺ doped TiO₂ is more active than un-doped TiO₂ catalyst with an efficiency of 99% for the nitrobenzene degradation at 120 min with an apparent rate constant of $35 \times 10^{-3} \text{ min}^{-1}$.

Keywords: Doped titanium dioxide, nanostructure, photocatalysis and nitrobenzene.

Resumen. La fotocatalisis es un método ampliamente utilizado en la degradación de contaminantes orgánicos del medio ambiente. El desarrollo de nuevos materiales es muy importante para proporcionar mejoras respecto a las propiedades fotocatalíticas y encontrar nuevas aplicaciones para TiO₂ como fotocatalizador. En este artículo se reporta la síntesis de un fotocatalizador a base de TiO₂ dopado con iones Zn²⁺ altamente eficiente para la degradación fotocatalítica de nitrobenzeno. Los resultados de las pruebas de actividad fotocatalítica mostraron que TiO₂ dopado es más activo que TiO₂ con una eficiencia del 99% para la degradación de nitrobenzeno en 120 min y una constante de velocidad aparente de $35 \times 10^{-3} \text{ min}^{-1}$.

Palabras clave: Dióxido de titanio dopado, nanoestructura, fotocatalizador, nitrobenzeno.

Introduction

Nitrobenzene (NB) is a carcinogenic pollutant widely used in the production of different products such as dyes, explosives and pesticides [1]. It is frequently released in the effluent from explosives manufacturing industry as well as in the manufacturing of organic chemicals and plastics [2]. Even at low concentrations NB can involve high risks to ecological and human health [3]. Continuous exposure of humans and animals to NB can result in methemoglobinemia and liver and kidney damage [4]. The US Environmental Protection Agency (US EPA) stipulates that wastewater with NB concentrations exceeding 2 mg L^{-1} is proclaimed as hazardous waste [5]. Owing to the strong electron affinity of the nitro group of NB, it is resistant to chemical or biological oxidation [6]. Meanwhile, a variety of possible treatment technologies, such as adsorption [7], photochemical reduction [8], oxidation by O₃/UV processes [9] and ozonation [10] have been adopted to remove NB from aqueous media. Another set of techniques relatively newer, more powerful and very promising are called Advanced Oxidation Processes (AOPs) which are been developed and employed to the treatment of contaminated wastewater effluents [11]. Photocatalytic degradation has proven to be a promising technology for removal of organic compounds [12]. This technique is more effective as compared to other AOPs because semiconductors are inexpensive and can easily mineralize various organic compounds [13, 14]. The basics steps for heterogeneous photocatalysis consist initially in transferring of the reactants in the

liquid phase onto the catalyst surface followed by adsorption of the reactant on the catalyst surface, reaction in the adsorbed phase, desorption of the final product and finally the removal of the final products in the liquid phase [15]. The development of photocatalysis has been the focus of considerable attention in recent years with photocatalysis being used in a variety of products across a broad range of research areas, including especially environmental and energy-related fields [16]. From several semiconductors used in photocatalysis, titanium dioxide (TiO₂) is one of the most important photocatalyst for the degradation of pollutants in water. This is because of its high photocatalytic activity, non-toxicity, chemical stability under different conditions and it is relatively inexpensive [17]. The photocatalytic properties of TiO₂ are derived from the formation of photo-generated charge carriers (hole and electron), which occurs due to the absorption of ultraviolet (UV) light corresponding to the band gap [16]. The photogenerated holes in the valence band diffuse to the surface of TiO₂ and react with adsorbed water molecules, forming hydroxyl radicals ($\bullet\text{OH}$) [18]. The photogenerated holes and the hydroxyl radicals oxidize nearby organic molecules on the surface of TiO₂. Meanwhile, electrons in the conduction band typically participate in reduction processes, and react with molecular oxygen to produce superoxide radical anions (O₂ \bullet^-) [19]. However, because of its large band gap (3.2 eV), it cannot absorb sunlight successfully. To reduce the band gap and increase the photoactivity of TiO₂ various ways have been tested, including the doping with different metal ions and oxides [20]. ZnO is a main semiconductor for

the synthesis of visible-light-active photocatalyst [21]. The results showed that coupled semiconductor photocatalysts were a novel approach to achieve a more efficient charge separation, an increased lifetime of the charge carriers and an enhanced interfacial charge transfer to adsorbed substrates. At the same time, their physical and optical properties are greatly modified [21]. Doping of TiO₂ with Zn²⁺ ions has been reported by Devi et. al. they described that dopants with lower charge than Ti⁴⁺ can alter the concentration of oxygen vacancies depending on their position in the TiO₂ matrix, they can replace Ti in TiO₂ lattice or can occupy interstitial position which in turn depends on their size and concentration. The Zn²⁺ ions decrease the recombination rate of the electro-hole pair, because zinc ions act as an electron acceptor in the conduction band reducing to Zn⁺, and with the holes they oxidize to Zn²⁺ increasing the generation of O₂•- and •OH radicals [15]. For this reason the main objective of the present study was to evaluate the photocatalytic activity of TiO₂ doped with Zn²⁺ ions in the degradation of a resistant pollutant as NB. In this work we report the synthesis of TiO₂ doped with zinc ions by the sol-gel method, the physical characterization and the photocatalytic results.

Results and Discussions

Characterization of photocatalyst

X-Ray diffraction

The crystalline nature and phase purity of nanocrystalline TiO₂ photocatalysts treated by thermal annealing at 600 °C were analyzed by X-ray powder diffraction. Fig. 1 shows the XRD patterns of the synthesized TiO₂ photocatalysts. All samples including pure TiO₂ photocatalyst reveals a pure anatase crystalline phase. Nadochenko et. al. reported that the transition of anatase to rutile phase is around 700 °C [22]. Tayade et. al. reported the synthesis of TiO₂ at different temperatures of calcination finding that at 640 °C, and higher, the rutile phase is

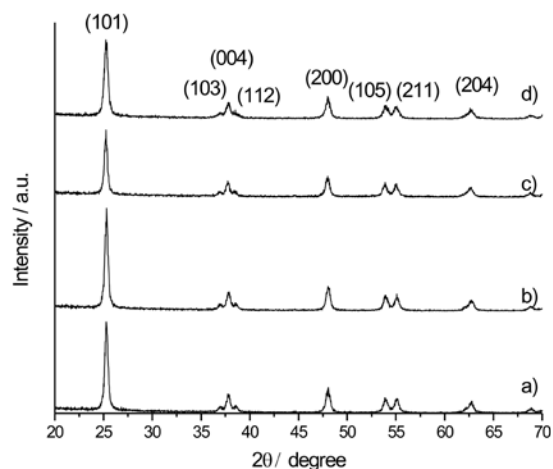


Fig. 1. XRD of photocatalyst: a) TiO₂, b) TiO₂- Zn 0.10, c) TiO₂-Zn 0.25, and d) TiO₂-Zn 0.50.

present [23]. In every one of the XRD patterns five peaks were observed at 25.3°, 36.6°, 48.0°, 54.5° and 62.6° in the 2θ range, which are indexed to the (101), (004), (200), (105) and (204) lattice d-spaces reflections of the TiO₂ anatase phase (JCPDS Card no. 21-1272) and no other crystalline phase is detected nor displacement in the 2θ angle. The XRD pattern does not present displacements in the 2θ, because structural changes by doping are strongly dependent of charge and ionic radius of the dopant. The dopant with a lower charge than Ti⁴⁺ can alter the concentration of oxygen vacancies depending on their position in TiO₂ matrix; they can replace Ti in TiO₂ lattice or can occupy interstitial position which in turn depends on their size and concentration. Hence these ions can easily substitute Ti⁴⁺ ion in the TiO₂ lattice without distorting the pristine crystal structure, thereby stabilizing the anatase phase over a range of dopant concentrations [24]. It must be noted that even at the highest Zn contents (0.5 atomic %) no diffraction peaks can be seen at 32°, 34.8° and 36.3° assigned to the hexagonal phase of the ZnO or displacement in the 2θ values [25].

The crystallite size, D, of the samples was estimated from the full-width at half maximum (β in radians) of the peak at 2θ = 25.4° by the Scherrer formula: $D = K\lambda / (\beta \cos \theta)$, K is a constant (0.89), λ is the X-ray wavelength (0.1541 nm for Cu Kα). The crystal sizes of photocatalysts are presented in Table 1. Reduction in the particle size of doped catalyst, in comparison to the un-doped one, can be attributed to the substitution of Ti⁴⁺ ions for Zn²⁺ ions in the crystalline structures. This may be due to the fact that Zn²⁺ ions have an ionic radius of 0.60 Å, which is smaller than the ionic radius of 0.68 Å of Ti⁴⁺ then, the substitution of Ti⁴⁺ ions by Zn²⁺ ions causes the reduction of the crystal size. This substitution of tetravalent cations for divalent cations promotes oxygen vacancies which are desired in redox reactions.

Transmission electron microscopy

TEM analysis revealed the morphology of the nanocrystalline TiO₂ photocatalyst. Fig. 2 shows bright field TEM images; all samples have regular homogeneity and a change in the particle size can be noticed also, the particles presents a spherical shape with variation in size due to the aggregation of small particles to form large particle conglomerates. Similar observations were made by Daimei et al. and Guangqin et al. when TiO₂ is doped with different ions [26, 27].

The Zn content in the samples was determined by energy dispersive X-ray spectroscopy (EDS) at different magnifications, using the STEM mode. The Fig. 3 shows the analysis area

Table 1. Crystal sizes of photocatalysts.

Catalyst	Crystal size (nm)
TiO ₂	20
TiO ₂ -Zn0.10	19
TiO ₂ -Zn0.25	18
TiO ₂ -Zn0.50	16

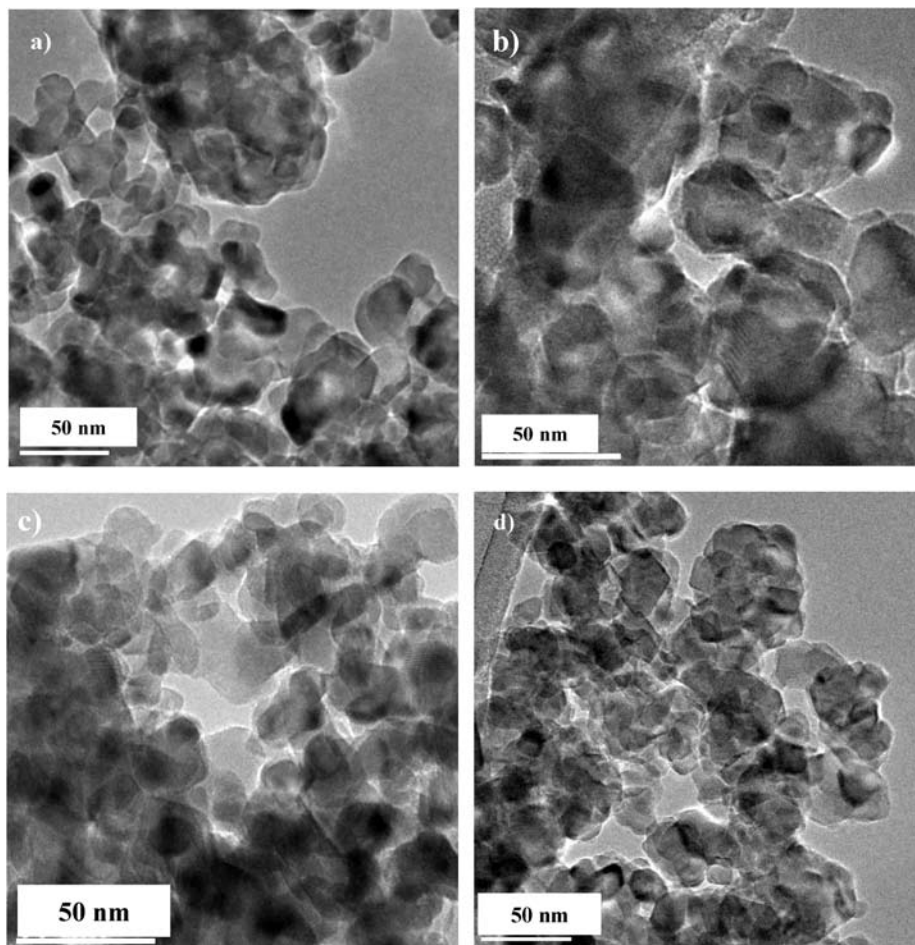


Fig. 2. TEM images of: a) TiO₂, b) TiO₂-Zn 0.10, c) TiO₂-Zn 0.25, and d) TiO₂-Zn 0.50.

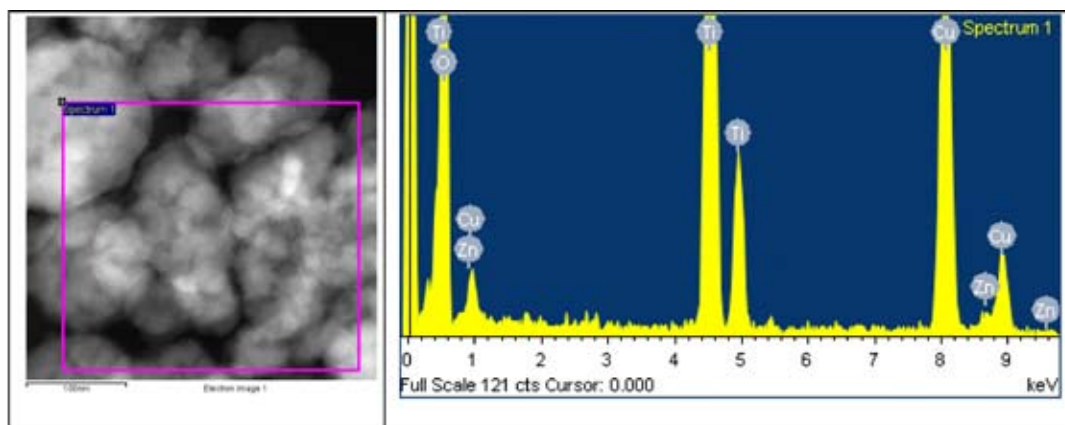


Fig. 3. EDS elemental analysis, area analysis content Zn, Ti and O.

and its respective spectrum, the quantities are 43.3, 56.54 and 0.16 atomic % for Ti, O and Zn respectively, the ratio between Zn and Ti is 0.4, which is close to the nominal ratio (0.5).

At the same time an elemental mapping was made using the same technique to determinate elemental distribution. Fig. 4 shows uniform distribution of Ti, O and Zn.

Raman spectroscopy

Titanium dioxide has frequently been investigated by Raman spectroscopy because of the unusual broadening and shifts of the bands with decreasing particle size. According to the factor group analysis, anatase phase has six Raman active modes (A_{1g}

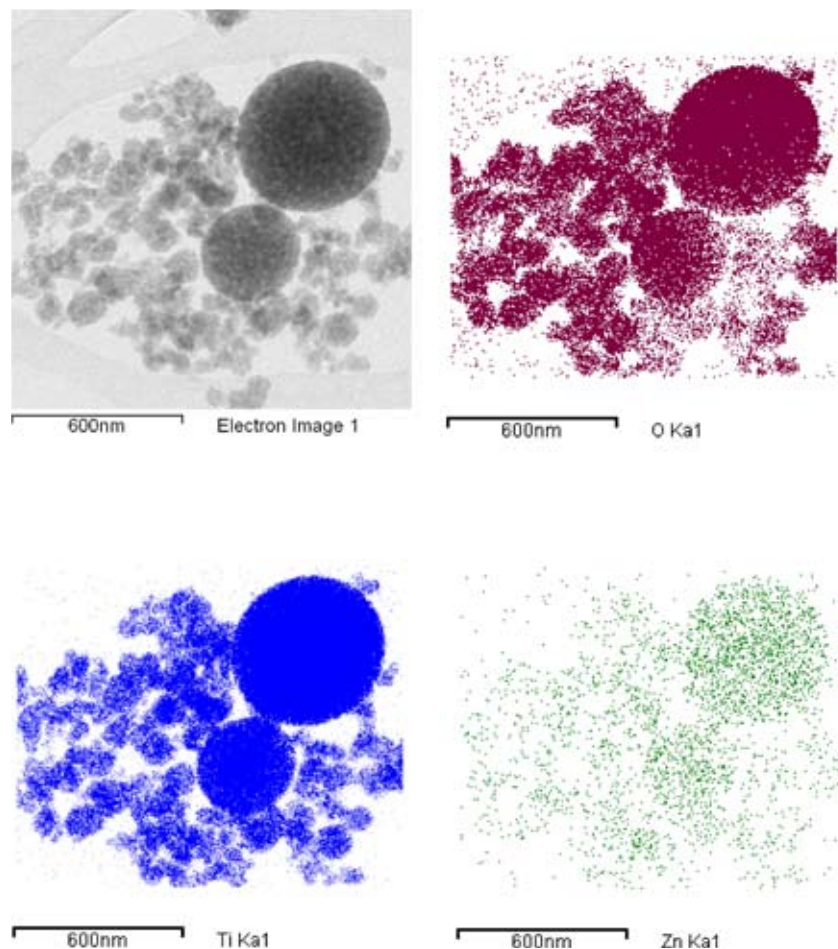


Fig. 4. EDS elemental mapping, Zn has a uniform distribution.

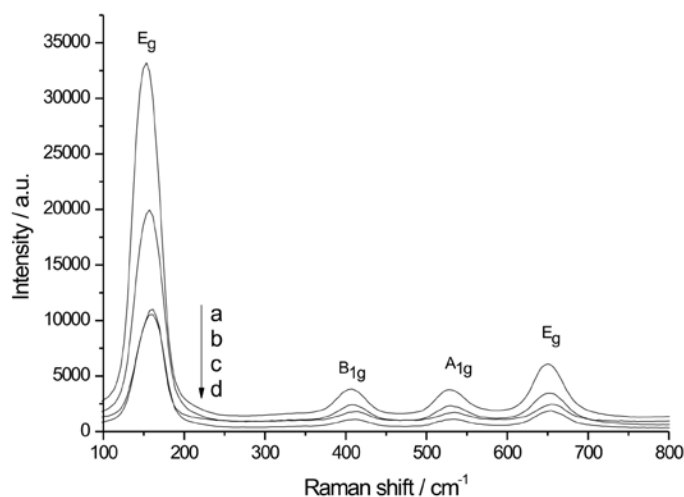


Fig. 5. Raman spectra of a) TiO₂, b) TiO₂-Zn 0.10, c) TiO₂-Zn 0.25, and d) TiO₂-Zn 0.50.

+ 2B_{1g} + 3E_g). Arsov *et al.* [28] studied the Raman spectrum of bulk single anatase crystal and concluded that the active Raman modes appears at 144 cm⁻¹ (E_g), 399 cm⁻¹ (B_{1g}), 516 cm⁻¹ (A_{1g}), and 639 cm⁻¹ (E_g).

The Raman spectra of nanocrystalline TiO₂ photocatalysts doped with zinc ions obtained in the 100 to 1000 cm⁻¹ region are shown in Fig. 5. All Raman spectra show the bands that are assigned to the modes of anatase TiO₂ but with a shift of the signals. The dominant band, assigned to the E_g mode, is centered at 152 cm⁻¹ and this shift is related to the change in the particle size. Bands centered at 406 and 528 cm⁻¹ are associated with B_{1g} and A_{1g} modes and the 648 cm⁻¹ band is assigned to E_g. In the Zn doped TiO₂, the B_{1g} mode exhibits a slight shift to higher wavenumbers. Because the B_{1g} mode comes from stretching of Ti-O bonds, this slight change is attributed to the substitution of Ti ions with Zn ions [29].

In order to analyze more clearly the differences between the spectra, the wavenumbers and the full-widths at half-maximum (FWHM) of the bands are presented in Table 2. Comparing the four Raman spectra, it is clear that the Raman bands shift towards higher wavenumber and their relative intensities decrease as the size of the particle decreases, generating oxygen vacancies changing the electronic properties of photocatalysts by the zinc ions content. These results are consistent with those obtained by XRD, where the smallest crystallite size corresponds to the samples with the highest content of Zn.

Table 2. The wavenumber and the FWHM (in parentheses) of the samples (cm^{-1}).

Catalyst	E_g	B_{1g}	A_{1g}	E_g
TiO_2	153.04 (41.1)	406.22 (35.2)	528.89 (41.1)	648.24 (46.1)
$\text{TiO}_2\text{-Zn0.10}$	158.17 (37.2)	409.38 (46.7)	530.39 (43.1)	653.06 (43.1)
$\text{TiO}_2\text{-Zn0.25}$	159.28 (37.2)	14.14 (33.3)	532.28 (47.1)	654.33 (45.0)
$\text{TiO}_2\text{-Zn0.50}$	161.03 (37.2)	411.04 (37.2)	533.71 (39.1)	656.23 (43.1)

Point of Zero Charge (PZC) by Zeta potential measurement

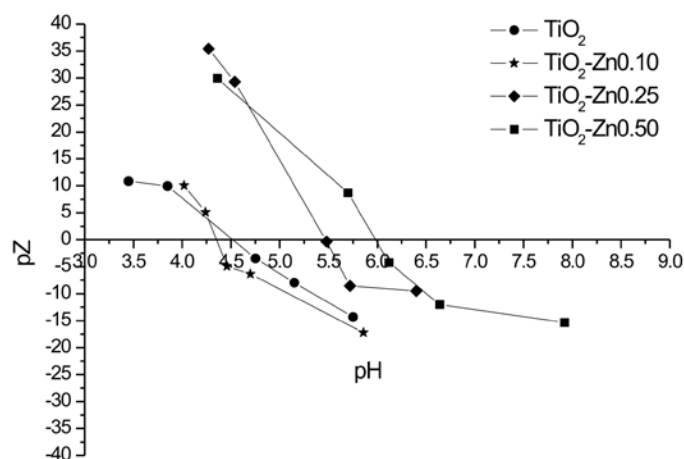
The PZC of an oxide is the value of pH at which the surface charge is zero. The knowledge of PZC is useful to predict whether ion exchange occurs preferentially to a specific component of the oxide system influencing the photoreactivity of the powder. Since photocatalysis occurs at the surface, the photocatalyst performance is highly affected by the pH of the solution, type of pollutant and the ability of the surface to adsorb it. Zeta potential of TiO_2 and Zn^{2+} -doped TiO_2 photocatalyst was measured as a function of pH (Fig. 6). The results show that in acidic or basic conditions, the surface of TiO_2 can respectively become positively or negatively charged [30]. The value of pH_{pzc} of the TiO_2 doped samples may be observed in Figure 6; for pH values smaller than pH_{pzc} the surface becomes positively charged and for pH values greater than pH_{pzc} the TiO_2 surfaces become negatively charged.

Photocatalytic activity

The efficiency of the photocatalysts was evaluated in the degradation of NB, studying the effect of dopant concentration and the pH of the solution under UV light at $\sim 25^\circ\text{C}$. The NB was selected as model pollutant because of its extensive use in industrial processes.

Effect of concentration of dopant

The degradation kinetics was computed by the change in the

**Fig. 6.** Zeta potential measurements of TiO_2 samples.

NB concentration employing UV-visible spectrometry as function of irradiation time. Figure 7 summarizes the effect of Zn^{2+} dopant concentration on the degradation efficiencies of NB solution as a function of irradiation time. The experimental results revealed that the photodegradation efficiency increases with the doping amount. The apparent rate constants of NB degradation are presented in the Table 3. It was found that the TiO_2 photocatalyst containing Zn^{2+} ions enhances the photocatalytic activity for the degradation of NB.

The photodegradation efficiency of un-doped TiO_2 was 70%, but when TiO_2 is doped with Zn^{2+} at 0.10, 0.25 and 0.50 atomic %, the photodegradation efficiency increase to 85, 94 and 97%, respectively.

TiO_2 is an effective photocatalyst that produces electrons and positive holes with UV irradiation, where TiO_2 acts as reductor agent and as oxidant. The change in the apparent degradation rate constant of NB can be explained by the presence of zinc ions in very small amounts, which we assume can easily substitute Ti^{4+} ions in TiO_2 lattice. The inclusion of Zn^{2+} ions modified the electron-hole pair recombination rate and oxygen vacancies, increasing the generation of $\text{O}_2^{\cdot-}$ and $\cdot\text{OH}$ radicals. The hydroxyl radicals are strong oxidant agents and these are formed by the adsorption of hydroxyl ions or water molecules in the traps holes of TiO_2 . Moreover, oxygen molecules are adsorbed in the traps for electrons, this leads to the formation of superoxide species then, by increasing the amount of zinc, the adsorption of water or oxygen molecule in trapping sites of carriers may be increased, which prolongs the lifetime of carriers, thereby improving the photocatalytic activity.

Effect of pH in the photodegradation of nitrobenzene

An important parameter in photocatalytic reactions is the pH of the solution since it dictates the surface charge of the photocatalyst, the size of the particle aggregates formed; the chemical nature of the pollutant and therefore its adsorption behavior [31, 32]. The interpretation of the pH effects on the degradation process is difficult as it includes various factors such as electrostatic interactions between the catalyst surface and reaction of charged radicals such as superoxide, hydroxyl radicals, etc. formed on the catalyst surface with pollutant molecules. The photocatalytic degradation of NB was carried out at pH 4, 7 and 10 at a fixed dose of TiO_2 doped with 0.5 atomic % of zinc ions. Figure 8 summarizes the effect of pH in the degradation efficiency of NB as a function of irradiation time. It can be seen that removal is quite high under acidic pH and is negligible under alkaline condition. This may be due to the fact that, under

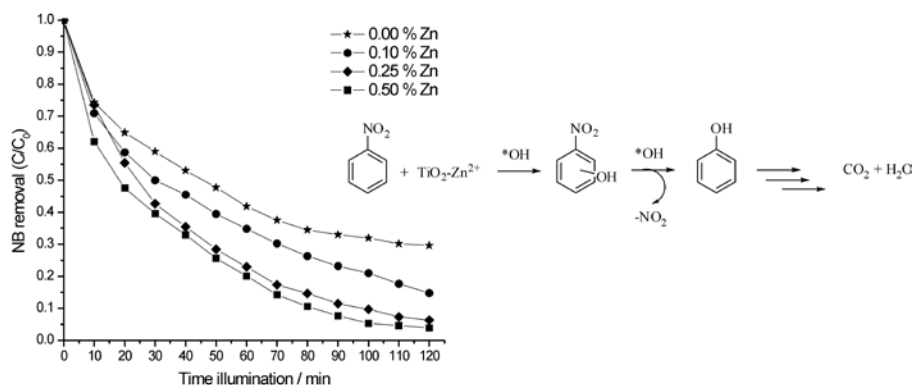


Fig. 7. Effect of the concentration of doping agent in the photocatalytic activity.

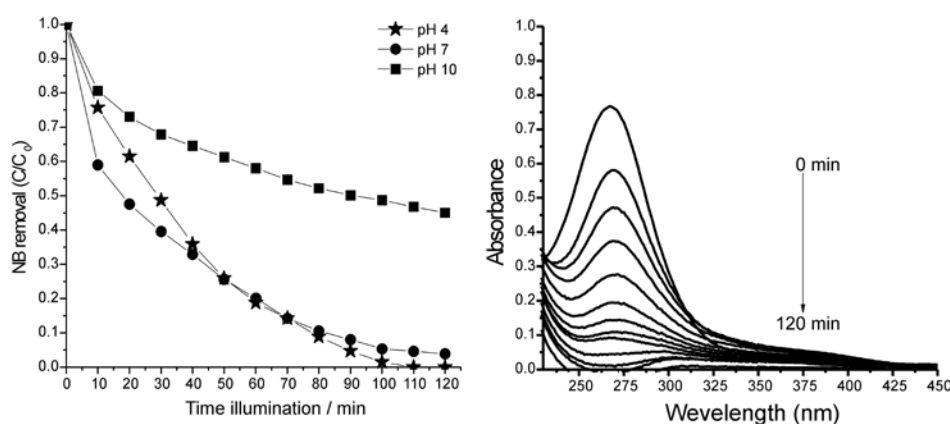


Fig. 8 a) Effect of pH in the photocatalytic degradation of nitrobenzene with nanocrystalline TiO₂ catalyst doped with 0.5 % of zinc ions and b) Evaluation of the degradation of NB under pH 4.

acidic pH, TiO₂ doped with zinc ions behaves as a strong Lewis acid due to the surface positive charge, according to the Zeta Potential. The NB is an aromatic compound with π electrons which can easily form a stable complex by donating electrons to the vacant d orbital of titanium [33]; in other words NB is a strong Lewis base and can easily adsorb on the positively charged catalyst surface. The efficiencies of NB degradation at pH 4, 7 and 10 are 99, 90 and 50%.

The apparent rate constants of the NB photodegradation reaction are shown in Table 4. The decrease in the rate of reaction at pH =10 may be due to two factors: competitive adsorption between hydroxyl ions and NB molecules, and Coulombic repulsion between the negatively charged catalyst and the NB molecules. From Fig. 8b it can be observed that the absorption band of NB at 266 nm decreases with the irradiation time

Table 3. Effect of dopant amount in the degradation rate.

Catalyst	Amount of Zn	Rate constant $\times 10^{-3} \text{ min}^{-1}$
TiO ₂	0.00 atomic %	7.6
TiO ₂ -Zn0.10	0.10 atomic %	14.4
TiO ₂ -Zn0.25	0.25 atomic %	22.7
TiO ₂ -Zn0.50	0.50 atomic %	26.9

Table 4. Effect of pH in the photocatalytic degradation rate of nitrobenzene with nanocrystalline TiO₂ doped with 0.5 % of zinc ions.

pH	Rate constant $\times 10^{-3} \text{ min}^{-1}$
4	35.7
7	26.9
10	5.8

in the presence of TiO₂ photocatalyst doped with 0.5 atomic % of Zn²⁺ ions, without the apparent formation of any other absorption band related to the formation of any by-product; under the oxidative reaction conditions, electrophilic hydroxyl radicals are the predominant species and can produce isomeric nitrophenols, isomeric diphenols by denitration of nitrophenols isomers, also can be formed phenol and these by-products can oxidize to carbon monoxide [34].

Conclusions

We have successfully prepared a highly efficient photocatalyst for the degradation of NB. The substitution of Ti⁴⁺ ions by Zn²⁺ ions in the anatase crystalline structure of TiO₂ increases the

photocatalytic activity; a possible explanation is that this substitution promotes the formation of p-n junction in $\text{TiO}_2\text{-Zn}^{2+}$, since the Zn ions can trap the generated holes in the valence band of TiO_2 avoiding the recombination of photogenerated electron-hole pairs by the inner electric field; this increases the degradation rate of NB and the photocatalytic activity. Also it was determined that at a low doping concentration of 0.5 atomic % the degradation of NB is more efficient. The acidic medium increases the adsorption of nitrobenzene in the surface of photocatalyst enhancing nitrobenzene photodegradation rate. The progress of the NB degradation reaction was carried out by UV-Vis spectroscopy and this was made to determine the possible formed by products of the reaction and the reaction rate.

Experimental

Materials

All chemicals were used as received without further purification and were purchased from Aldrich. Zinc acetate dihydrate ($\text{Zn}(\text{C}_2\text{H}_3\text{O}_2)_2 \cdot 2\text{H}_2\text{O}$), titanium tetraisopropoxide (TTIP), Ammonium hydroxide (NH_4OH), Acetonitrile (CH_3CN), 2-propanol ($\text{C}_3\text{H}_8\text{O}$) and Nitrobenzene ($\text{C}_6\text{H}_5\text{NO}_2$).

Synthesis of nanocrystalline TiO_2 photocatalysts doped with zinc ions

The synthesis of nanocrystalline TiO_2 photocatalysts doped with different amounts of zinc (0.10, 0.25 and 0.50 atomic %) was made by the sol-gel method. Zinc acetate dihydrate was used as a doping starting material and titanium tetraisopropoxide (TTIP) as the titanium source. The molar amount of zinc ion was calculated in order to substitute 0.10, 0.25 and 0.50 atomic % of titanium ions and NH_4OH was used for the hydrolysis reactions. The procedure was as follows: 0.0198 moles of TTIP were dissolved in 50 mL of isopropanol and 240 mL of acetonitrile followed by the addition of 5 mL of aqueous solution of $\text{Zn}(\text{C}_2\text{H}_3\text{O}_2)_2 \cdot 2\text{H}_2\text{O}$ with the appropriate concentration for the substitution of 0.10, 0.25 and 0.50 atomic % of titanium ions, and left to react for 30 min. at 40 °C and constant magnetic stirring. After this reaction time the mixture was cooled at room temperature at constant stirring and 5 mL of NH_4OH 0.33 M aqueous solution was added forming a white suspension. The resulting suspension was maintained at room temperature for 60 min, filtered and washed with deionized water. The white solid of zinc-ion-doped TiO_2 photocatalysts were treated at 600 °C for 6 h in air. The un-doped TiO_2 photocatalyst was prepared using the same procedure, without the addition of the doping metal precursor, for comparative purposes.

Characterization of nanocrystalline TiO_2 photocatalyst

Several techniques were used to characterize the nanocrystalline TiO_2 photocatalysts doped with zinc ions. The XRD patterns were collected with a Philips X-pert MPD diffractometer

with Cu $K\alpha$ radiation, operated at 43 kV and 30 mA; the samples were scanned with steps of 0.02° and 0.2 s of collection per step. TEM analysis was performed with a JEOL 2010 at an acceleration voltage of 200 kV. The samples for TEM analysis were prepared by ultrasonic dispersion of nanocrystalline photocatalysts in methanol for about 2 min. Then, a drop of the dispersion was placed on a copper grid coated with a holey carbon film. The Raman spectra were recorded on Xplora spectrometer (HORIBA-JobinYvon) equipped with diode laser of 532 nm wavelength. Zeta potential as function of pH was measured by dynamic light scattering spectrophotometer (Zetasizer instrument, Malvern Co., U. K.). 2 mg of the samples were dispersed in 30 g of distilled water and ultrasonicated prior to measurement. The pH of colloidal solutions was controlled by the addition of HCl (0.1 M) or NaOH (0.1 M).

Photocatalysis experiments

Photocatalytic degradation experiments were carried out in a photochemical reactor Rayonet model RPR100, which was modified in order to have magnetic stirring. The photocatalytic experiments of nitrobenzene degradation were performed in a cylindrical quartz cell with a total volume of 170 cm³ of nitrobenzene solution at 15 mg L⁻¹ under UV irradiation with UV lamps of 300 nm at temperature ~25 °C; the temperature was controlled by recirculation of the solution in a Liebig condenser. Photodegradation efficiency was determined by plotting of C/C_0 vs irradiation time (min), where C_0 and C are the nitrobenzene concentrations at zero time and time t , respectively. The value of C/C_0 was taken as the ratio A/A_0 , i.e. the absorbance value of the solution at λ_{max} at time t divided by the absorbance at time zero. NB exhibits strong absorption band at 266 nm, the change in the intensity absorbance was followed by UV-Vis spectroscopy using a Varian model 100 Bio spectrophotometer. Samples of 3 mL were taken from the NB solution after a specific time interval and analyzed. The apparent rate constant (K_{app}) was determined by plotting $\ln C/C_0$ versus time during the first 60 min of irradiation.

Acknowledgements

We thank the Dirección General de Educación Superior Tecnológica (DGEST), Grant No. 2534.09-P, PROMEP project PROMEP/103.5/13/8162 and CONACyT project 175925 for their support of this investigation. We also thank to R. Somanthan, F. Ruiz and E. Aparicio for their technical support.

References

1. Mu, Y.; Rozendal, R. A.; Rabaey, K.; Keller, J. *Environ. Sci. Technol.* **2009**, 43 (22), 8690.
2. Ikeda, M.; Kita, A. *Br. J. Ind. Med.* **1964**, 21, 210.
3. Wang, X. L.; Li, Y.; Wang, Y. Z.; Wang, T.; Gao, Q.; Du, X. Y. *China J. Hazard. Mater.* **2009**, 172, 755.
4. Zheng, C.; Zhou, J.; Wang, J.; Wang, J.; Qu, B. *J. Hazard. Mater.*

- 2008, 160, 194.
5. EPA, *Nitroorganic and Nitroamines by High Performance Liquid Chromatography (HPLC)*, 8300 Method, USA, 1994.
 6. Rodgers, J. D.; Bunce, N. J. *Water Res.* **2001**, 35, 2101.
 7. Boyd, S. A.; Sheng, G. Y.; Teppen, B. J.; Johnston, C. T. *Environ. Sci. Technol.* **2001**, 35, 4227.
 8. Makarova, O. V.; Rajh, T.; Thurnauer, M. C.; Martin, A.; Kemme, P. A.; Crokek, D. *Environ. Sci. Technol.* **2000**, 34, 4797.
 9. Latifoglu, A.; Gurol, M. D. *Water Res.* **2003**, 37, 1879.
 10. Beltrán, F. J.; Encinar, J. M.; Alonso, M. A.; *Ind. Eng. Chem. Res.* **1998**, 37, 25.
 11. Rauf, M.A.; Ashraf, S.S., *Application of Advanced Oxidation Processes (AOP) to dye degradation—an overview*, Lang, A. R. (Ed.), *Dyes and Pigments: New Research*, Nova Science Publishers, Inc, **2009**.
 12. Forgacs, E.; Cserhádi, T.; Oros, G. *Environ. Int.* **2004**, 30, 953.
 13. Stylidi, M.; Kondarides, D. I.; Verykios, X. E. *Appl. Catal. B* **2003**, 40, 271.
 14. Guzsván, V. J.; Csanádi, J. J.; Lazic, S. D.; Gaál, F. F. *J. Braz. Chem. Soc.* **2012**, 20, 152.
 15. Rauf, M.A.; Meetani, M.A.; Hisaindee, S. *Desalination* **2011**, 276, 13.
 16. Fujishima, A.; Zhang, X.; Tryk, D. A. *Surf. Sci. Rep.* **2008**, 63, 515.
 17. Tian, J.; Chen, L.; Dai, J.; Wang, X.; Yin, Y.; Wu, P. *Ceram. Int.* **2009a**, 35, 2261.
 18. Sirtori, C.; De Freitas, A. M.; Fujiwara, T.; Peralta, P. *J. Braz. Chem. Soc.* **2012**, 23, 1563.
 19. Nakata, K.; Fujishima, A. *J. Photochem. Photobiol. C* **2012**, 13, 169.
 20. Chen, C.; Wang, Z.; Ruan, S.; Zou, B.; Zhao, M.; Wu, F. *Dyes Pigm.* **2008**, 77, 204.
 21. Khan, R.; Kim, T. J. *J. Hazard. Mater.* **2009**, 163, 1179.
 22. Bacsa, R.; Kiwi, J.; Ohno, T.; Albers, P.; Nadtochenko, V. *J. Phys. Chem. B* **2005**, 109, 5994.
 23. Tayade, R. J.; Kulkarni, R. G.; Jasra, R. V. *Ind. Eng. Chem. Res.* **2006**, 45, 922.
 24. Gomathi, L.; Kottam, N.; Narashimha, B.; Murthy, S.; Kumar, G. *J. Mol. Catal. A: Chem.* **2010**, 328, 44.
 25. Jang, J. S.; Yu, C. J.; Choi, S. H.; Ji, S. M.; Kim, E. S.; Lee, J. S. *J. Catal.* **2008**, 254, 144.
 26. Daimei, C.; Zhongyi, J.; Jiaqing, G.; Qun W.; Dong Y. *Ind. Eng. Chem. Res.* **2007**, 46, 2741.
 27. Guangqin, L.; Chunyan, L.; Yun, L. *Appl. Surf. Sci.* **2006**, 253, 2481.
 28. Arsov, L. D.; Kormann, C.; Plieth, W. *J. Raman Spectrosc.* **1991**, 22, 573.
 29. Mengjin, Y.; Chad, H.; Sangwook, L.; You-Hwan, S.; Jung-Kun, L.; *J. Phys. Chem. C* **2010**, 114, 15292.
 30. Jianjuan, L.; Shiwei, L.; Li, Z.; NengQian, P.; Xiankun, C.; Jianbao, L. *ACS Appl. Mater. Inter.* **2012**, 4, 171.
 31. Araújo, A. B.; Amarante, O. P.; Vieira, E. M.; Valente, J. P. S.; Padilha, P. M.; Florentino, A. O. *J. Braz. Chem. Soc.* **2006**, 17, 737.
 32. Gupta, V. K.; Jain, R.; Mittal, A.; Saleh, T. A.; Nayak, A.; Agarwal, S.; Sikarwar, S. *Mat. Sci. Eng. C* **2012**, 32, 12.
 33. Lachheb, H.; Puzenat, E.; Houas, A.; Ksibi, M.; Elaloui, E.; Guillard, C.; Herrmann, J. M. *Appl. Catal., B* **2002**, 39, 75.
 34. Shu-Juan, Z.; Hong, J.; Min-Jie, L.; Han-Qing, Y.; Hao, Y.; Qian-Rong, L. *Environ. Sci. Technol.* **2007**, 41, 1977.